

# Comparison of various growth curve models in characterizing and predicting water table change after intensive mine dewatering is discontinued in an East Central European karstic area

Kamilla Modrovits, András Csepregi, Ilona Kovács Székely, István Gábor Hatvani\*, and József Kovács

Correspondence: hatvaniig@gmail.com

**Table S1.** List of acronyms and abbreviations

<b>K</b>	<b>maximum water level value</b>
<b>m asl.</b>	<b>meters above sea level</b>
<b>Fm</b>	<b>Formation</b>
<b>SW</b>	<b>southwest</b>
<b>NE</b>	<b>northeast</b>
<b>Jan</b>	<b>January</b>
<b>LDA</b>	<b>linear discriminant analysis</b>
$\lambda$	<b>Wilks's lambda quotient</b>
<b>r, r<sup>2</sup></b>	<b>correlation index, square of correlation index</b>
<b>CRAE</b>	<b>complementary relationship areal evapotranspiration</b>
$\gamma(h)$	<b>semivariogram</b>
<b> h </b>	<b>planar distance</b>
<b>N(h)</b>	<b>number of lag distance</b>
<b>c<sub>0</sub></b>	<b>nugget</b>
<b>c</b>	<b>sill</b>
<b>a</b>	<b>range</b>
<b>RSS</b>	<b>Residual Sum of Squares</b>
<b>Mts.</b>	<b>Mountains</b>
<b>y</b>	<b>measured value</b>
$\hat{y}$	<b>estimated value</b>
<b>SSE</b>	<b>Sum of Squared Errors</b>
<b>SST</b>	<b>Sum of Squares Total</b>

Section S1. Applied trend functions

In the karst aquifer of the Transdanubian Range, the recovery process has started after the water abstraction stopped, and still going on. It has a limited increase, as the expected water level values have an upper maximum. After ceasing the artificial effect, the water levels tend to return to the state of around the 1950s. To characterize the process different types of growth curves [1] can be used which approach a given constant -  $K$  maximum water level value - in time.

Formally:

$$f(t) = K$$

Two groups of this type of the growth curves were used. A significant type of these functions does not have an inflection point and have a concave run in the domain of  $0 - \infty$  (Figure S1).

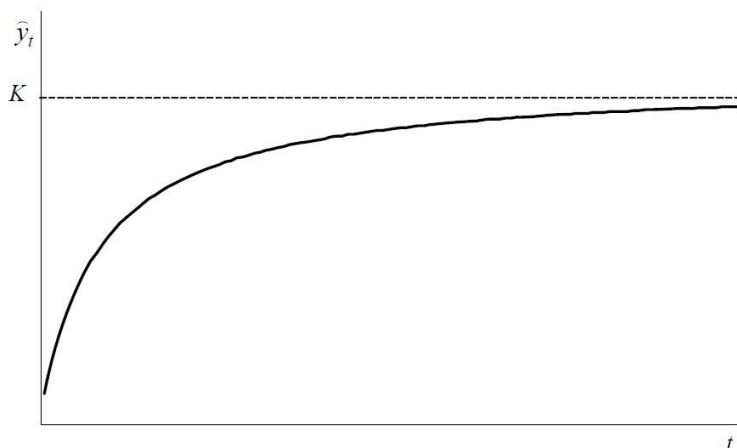


**Figure S1.** Characteristic appearance of a growth curve without an inflection point, where  $t$ =time;  $\hat{y}_t$ = estimated value;  $K$ =maximum value [1]

This is true if the trend function can be derived twice according to the time variable and the second derivative is negative. Three of this type of functions were used in the study: Bertalanffy [2], Törnquist1 and Törnquist2 [3-4] (Table S2).

**Table S2.** The most important characteristics of growth curves without an inflection point ( $K$ =maximum value;  $t$ =time;  $a, b$ = function parameters)

Name	Formula	$\hat{y}_0$	$\frac{d^2\hat{y}_t}{dt^2}$	$\hat{y}_t$
<b>Bertalanffy</b>	$\hat{y}_t = K(1 - be^{-rt})$	$K(1-b)$	$-Kbr2e^{-rt}$	$K$
<b>Törnquist 1</b>	$\hat{y}_t = \frac{Kt}{t + a}$	$0$	$\frac{-Ka2}{a + t^3}$	$K$
<b>Törnquist 2</b>	$\hat{y}_t = \frac{K(t + a)}{t + b}$	$\frac{Ka}{b}$	$\frac{2K(a - b)}{b + t^3}$	$K$

There are processes showing an exponential rise initially, but over a longer period of time, exceeding a certain value (at the inflection point) the growth slows down, which can be properly described e.g. by a logistic curve [5]. This type of growth functions is also called sigmoid function. They have an inflection point, relative to which the initial section is concave, while the section after that is convex. The inflection point may indicate that there have been some significant changes in the process. From this point on, it can be interpreted as the “power” of the process, which has ceased. In

addition to the original logistic function, there are a number of mathematical functions with a similar shape. In this research, seven of these functions were examined.

In this study, the term of logistic trend function refers to the Pearl-Reed logistic curve [6] (Figure S2/A). The inflection point is at  $\frac{K}{2}$ , the curve is symmetric at this point. However, some processes are not best approximated by the original logistics function: the location of the inflection point and the shape of the function can be slightly different.

The change in the process rate does not necessarily occur at the half of the maximum value. In this case, the delayed logistic trend function can be used [7] (Figure S2/B), where the initial growth is faster but characterized by a more prolonged shape after reaching the inflection point, i.e. a delayed effect can appear in reaching the maximum level. The squared logistic trend function [8] (Figure S2/C) is the square of the classical logistic trend function, where the inflection point occurs later compared to the classical model. The Gompertz function [9] (Figure S2/D) can be used for processes characterized by a steep, rapid rise in the early - developmental stage, thus, it reaches the saturation level earlier than the classical function. The further development of this function results the double exponential function. In case of the '63 percent' trend function [8] (Figure S2/E), at time  $t = T$ , the function reaches 63% of the  $K$  maximum level, notably:

$$\hat{y}_T = K - \frac{K}{e} = K \left( 1 - \frac{1}{e} \right) = 0,632K$$

In the Johnson function [10] (Figure S2/F), the inflection point can be reached relatively quickly, followed by a long, slow-growing phase until the threshold level is reached. Richards [11] incorporated a  $v$  parameter into the model he had developed, with which the location of the inflection point can be controlled. In this function – widely accepted in the international literature – the value of the lower limit  $A$ , which characterizes the trend, has also been introduced, thus, the function does not have only a maximum but also a minimum value ( $A$ ) (Figure S2/G).

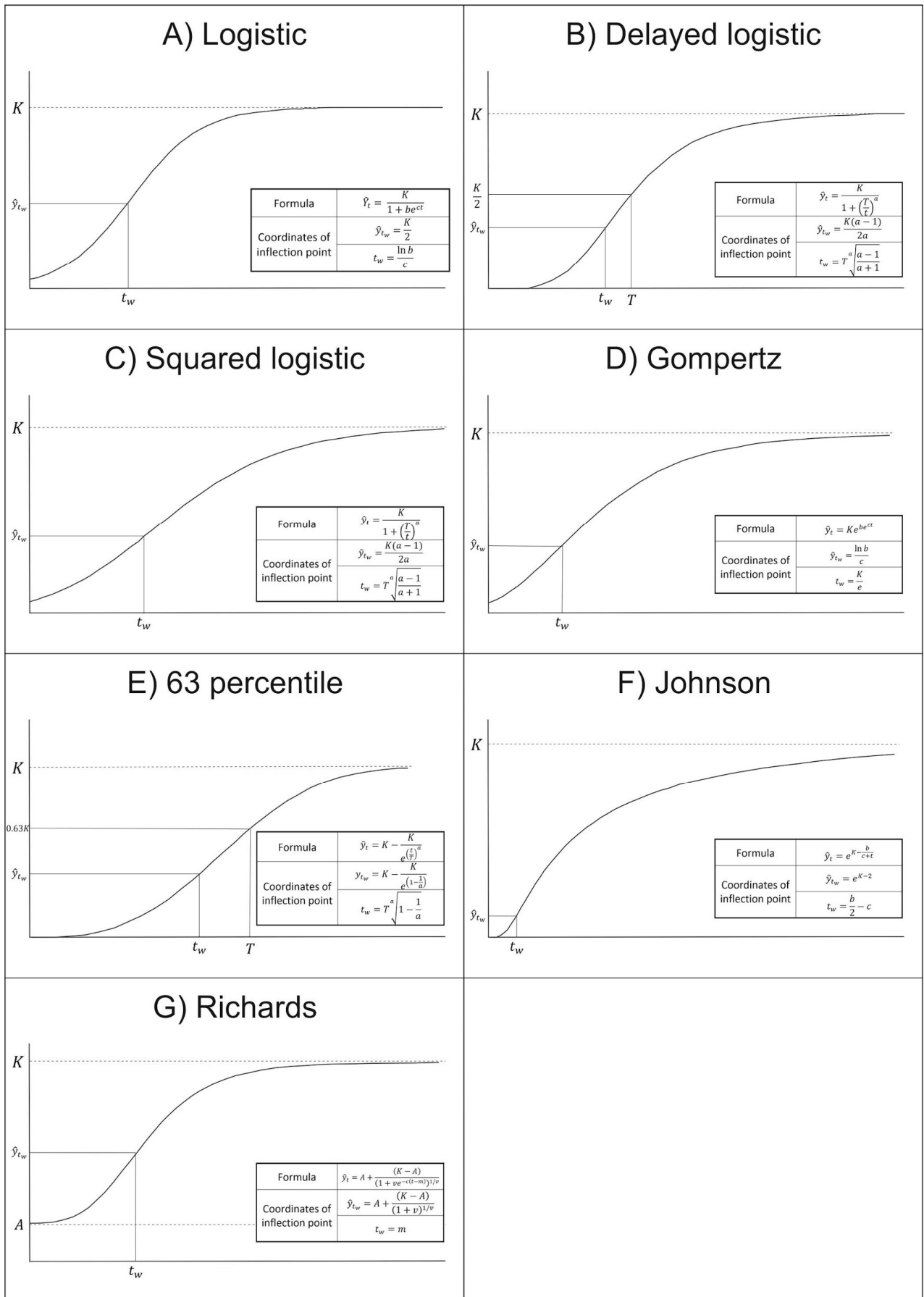


Figure S2. Functions with one inflection point and their characteristic points (after Kehl and Sipos [1])

Table S3. K (maximum water level) value estimation

Well	K based on map				Jan 2030			
	Bertalanffy	Delayed log.	'63 percent'	Richards	Bertalanffy	Delayed log.	'63 percent'	Richards
<b>Bakonybél-2a</b>		231.8			225.5	220.2	226.0	228.2
<b>Bakonyszentkirály-14</b>		175.8			168.7	170.5	175.8	176.3
<b>Csabdi-150</b>		145.0			129.9	126.5	130.6	134.1
<b>Csákberény-86/a</b>		161.1			151.0	151.5	156.1	156.7
<b>Duka-1</b>		177.6			175.6	171.5	175.6	176.7
<b>Epöl-5</b>		143.8			134.4	132.2	138.8	137.7
<b>Iszkaszentgyörgy Kp-248</b>		133.5			130.9	130.9	133.4	133.2
<b>Jásd-41a</b>		192.8			180.2	182.0	187.6	190.9
<b>Nyergesújfalu-30</b>		132.5			128.6	127.3	130.0	130.9
<b>Sólymár-97</b>		130.0			127.3	127.9	129.4	130.0
Well	Estimated K				Jan 2030			
	Bertalanffy	Delayed log.	'63 percent'	Richards	Bertalanffy	Delayed log.	'63 percent'	Richards
<b>Bakonybél-2a</b>	261.8	542.3	235.4	236.4	236.4	239.0	228.0	231.1
<b>Bakonyszentkirály-14</b>	519.1	590.2	380.2	183.0	187.3	192.3	193.0	176.3
<b>Csabdi-150</b>	161.0	465.8	144.7	131.6	132.5	133.7	130.5	128.2
<b>Csákberény-86/a</b>	333.9	335.3	264.6	160.4	168.1	170.3	171.2	156.2
<b>Duka-1</b>	170.8	179.4	168.2	165.5	170.0	172.3	168.0	165.5
<b>Epöl-5</b>	156.9	233.9	151.4	133.6	137.5	137.6	137.4	131.9
<b>Iszkaszentgyörgy Kp-248</b>	149.7	119.6	115.3	116.7	143.1	119.2	115.3	116.7
<b>Jásd-41a</b>	865.3	24815.3	5001.8	244.0	205.2	214.3	213.7	210.0
<b>Nyergesújfalu-30</b>	162.6	277.1	156.2	131.8	137.5	139.3	136.6	130.4
<b>Sólymár-97</b>	310.3	643.0	1130.6	138.2	135.7	139.2	140.3	135.0

## Section S2. Description of deterministic model

The deterministic model describing the recovery of the Transdanubian Range is a transient hydraulic model. Its mathematical background is a differential equation describing the groundwater flow:

$$\frac{\sigma}{\sigma x} \left( T \frac{\sigma h}{\sigma x} \right) + \frac{\sigma}{\sigma y} \left( T \frac{\sigma h}{\sigma y} \right) + \frac{\sigma}{\sigma z} \left( T \frac{\sigma h}{\sigma z} \right) = S \frac{\sigma h}{\sigma t} + q$$

where:

x, y, z: coordinates;

h: hydraulic head;

T: transmissivity;

S: storage;

q: the sum of the discharge and recharge (e.g. abstraction, evaporation) per unit area.

Applied Visual Modflow software solves the flow equation by finite difference method.

The model area is divided with along a constant orthogonal grid, the grid size is 500x500 m for the total model area. The time step of the transient model is one month. There are no-flow boundary conditions in the model along the main structures of the Transdanubian Range Unit. Considering the geological settings, only the Upper Triassic

strata, which gives the main mass of the aquifer, were included in the hydraulic model. Based on mining and deep drilling experiences in practice, it is assumed that the significant part of the groundwater flow occurs in the upper 150-200 meters of the karst aquifer. The vast majority of the wells does not explore the aquifer deeper than 50 - 100 m. Based on these information, the upper 200 m of the karst aquifer was built into the model. In areas where leakage is possible between the Triassic and the overlying aquifers (e.g., Cretaceous limestones, Upper Pannonian porous layers), the model calculates the water exchange between the two aquifers based on the hydraulic conductivity. The flow rate between the karst aquifer and surface waters was also calculated by the hydraulic model.

The model also includes the major karst springs, regarded as fixed drains in the model, where the hydraulic conductivity value was given for the finite difference mesh grid element which corresponds to the elevation. Based on the difference between the karst water level and the elevation of springs, their yield can be calculated. As a result of the recovery, the cold and lukewarm springs dried up decades ago restarted and the yield of the springs exceeded the amount of abstraction.

The renewable water supply of the dynamic karst aquifer is equal to the infiltration rate of the precipitation falling into the karst outcrops. The recharge is thus equal to the spatial characteristic of diffuse infiltration, which can be determined from the product of the open karstic infiltration and its intensity. For calculating the latter, rainfall measuring stations close to the infiltration areas were used. In Hungary in karstic areas surface runoff is negligible, precipitation is instrumentally measured, thus using the base-function of hydrology seepage can be determined by subtracting evapotranspiration - estimated using the Morton CRAE model [12] - from precipitation.

All yield values were transferred to the corresponding elements of the grid according to the EOVS coordinates of the water abstraction - as usual for the finite difference method used. Monthly karst water abstraction data were included in the model, as well.

The regionally updated database of the model allows the simulation of water level changes, yield changes of major karst springs in the karst reservoir from 1951 up to the present day. Furthermore, it is also suitable for predicting changes in the expected karst water level.

**Table S4.** Statistics of water level values predicted for Jan 2030 with different growth models (in 107 wells)

	<b>Bertalanffy</b>	<b>Törnquist1</b>	<b>Törnquist2</b>	<b>Logistic</b>	<b>Delayed log.</b>
<b>Mean</b>	159.940	153.666	153.589	165.361	157.900
<b>Median</b>	140.004	134.558	134.558	145.212	137.747
<b>Range</b>	170.9	170.7	169.5	182.0	173.0
<b>Interquartile range</b>	48.094	44.316	44.316	52.949	49.302
	<b>Squared log.</b>	<b>Gompertz</b>	<b>63 perc.</b>	<b>Johnson</b>	<b>Richards</b>
<b>Mean</b>	164.527	163.356	162.048	155.830	164.176
<b>Median</b>	144.245	142.980	141.296	136.706	142.980
<b>Range</b>	179.9	177.2	175.9	170.1	188.8
<b>Interquartile range</b>	52.859	52.367	52.259	45.876	50.935

## References

1. Kehl. D.; Sipos. B. A telítődési, a logisztikus és az életgörbe alakú trendfüggvények becslése Excel parancsfájl segítségével. *Statisztikai Szemle* 2009. 87(4). pp. 381–411.

2. Bertalanffy. L. A Quantitative Theory of Organic Growth (Inquiries on Growth Laws II.). *Human Biology* **1938**. 10(2). pp. 181-213.
3. Törnquist. L. The Bank of Finland's Consumption Price Index. *Bank of Finland Monthly Bulletin* **1936**. 16(10). pp. 27-32.
4. Törnquist. L. *Collected scientific papers of Leo Törnquist*. 1st ed.; The Research Institute of the Finnish Economy: Helsinki. Finland. 1981.
5. Verhulst. P.-F. Notice sur la loi que la population poursuit dans son accroissement. *Correspondance Mathématique et Physique* **1838**. 10. pp. 113–121.
6. Pearl. R.; Reed. L.J. On the Rate of Growth of the Population of the United States since 1790 and its Mathematical Representation. In *Mathematical Demography*; Smith. D.P., Keyfitz. N., Eds.; Springer-Verlag: Heidelberg. Germany. 1977; pp. 341-347.
7. Hutchinson G.E. Circular causal systems in ecology. *Annals of the New York Academy of Sciences* **1948**. 50(4). pp. 221-246. <https://doi.org/10.1111/j.1749-6632.1948.tb39854.x>
8. Kotz. S.; Johnson. N.L.; Read. C.B. *Encyclopedia of Statistical Sciences*. 2nd ed.; Wiley InterScience: New Jersey. USA. 2006.
9. Gompertz. B. On the Nature of the Function Expressive of the Law of Human Mortality. and on a New Mode of Determining the Value of Life Contingencies. *Philosophical Transactions of the Royal Society of London* **1825**. 115. pp. 513–585.
10. Johnson. N.L. Systems of frequency curves generated by methods of translation. *Biometrika* **1949**. 36. pp. 149–176.
11. Richards. F. J. A Flexible Growth Function for Empirical Use. *Journal of Experimental Botany* **1959**. 10(2). pp. 290–301. <https://doi.org/10.1093/jxb/10.2.290>
12. Morton. F.I. Operational estimates of areal evapotranspiration and their significance to the science and practice of hydrology. *Journal of Hydrology* **1983**. 66. pp. 1-76.